

Emission from neutral and charged excitons in a single quantum dot in a magnetic field

C. Schulhauser^{a,*}, R.J. Warburton^b, A. Högele^a, A.O. Govorov^c, K. Karrai^a,
J.M. Garcia^d, B.D. Gerardot^c, P.M. Petroff^e

^a*Sektion Physik und CeNS, Ludwig-Maximilians-Universität, Geschwister-Scholl-Platz 1, D-80539 München, Germany*

^b*Department of Physics, Heriot-Watt University, Edinburgh EH14 4AS, UK*

^c*Department of Physics and Astronomy, Ohio University, Athens, OH, USA*

^d*Instituto de Microelectronica de Madrid, CNM-CSIC Isaac Newton, 8 (PTM), 28760 Madrid, Spain*

^e*Materials Department, University of California, Santa Barbara, CA 93106, USA*

Abstract

We report on optical spectroscopy of self-assembled InAs quantum dots in a magnetic field. We describe how we measure the emission characteristics of a single quantum dot (QD) in high magnetic fields at low temperature using a miniature, fiber-based confocal microscope. Example results are presented on a QD whose charge can be controlled using a field-effect device. For the uncharged, singly and doubly charged excitons we find a diamagnetism and the spin Zeeman effect. In contrast, for the triply-charged exciton we find a fundamentally different behavior. Anti-crossings in magnetic field imply that confined states of the QD are hybridized with Landau-like levels associated with the two-dimensional continuum.

© 2003 Elsevier B.V. All rights reserved.

PACS: 78.67.Hc; 73.40.Rw; 78.66.Fd

Keywords: Spectroscopy; Quantum dot; Photoluminescence; Magnetic properties

1. Introduction

Quantum dots (QDs) in semiconductors have received an enormous amount of interest in the last few years. This is largely because the strong confinement of both electrons and holes in all three directions leads to discrete energy levels, not the bands typical of a semiconductor. This atom-like property can be exploited, for instance for a single-photon source [1].

Single-dot techniques have been shown to be very powerful for characterizing the electron and hole states as they remove the inhomogeneous broadening which plagues experiments on ensembles. The homogeneous broadening is only a few micro electron volt at low temperature for InAs/GaAs QDs [2]. Application of a magnetic field yields important information in inter-band spectroscopy. It is clearly desirable to perform magneto-spectroscopy on individual QDs. There are experimental difficulties in achieving this because in typical single dot setups, the collection area moves relative to the sample when a magnetic field is applied. We present here a novel low-temperature confocal microscope, which does not suffer from this problem.

* Corresponding author. Tel.: +49-89-2180-1457; fax: +49-89-2180-3182.

E-mail address: christian.schulhauser@physik.uni-muenchen.de (C. Schulhauser).

We present some example results on InAs/GaAs QDs embedded in a heterostructure, which allows the exciton charge to be changed controllably. The results determine the exciton g -factor, the extent of the wave function, and a surprising interaction with Landau levels for the triply charged exciton.

2. Experimental details

We use InAs/GaAs QDs in a vertical tunneling structure [3]. The self-assembled InAs QDs are grown by molecular beam epitaxy (MBE) on a GaAs substrate. A GaAs buffer is grown as starting material followed by a 20 nm thick highly n-doped layer using silicon as a donor with a concentration of $n_d = 4 \times 10^{18} \text{ cm}^{-3}$. The n-doped layer serves as a back contact for our field effect device. A 25 nm thick undoped GaAs layer follows the back contact and represents a barrier for electron tunneling from the back contact. The QDs themselves are then grown using self-assembly in the Stranski–Krastanov mode. At a coverage of 1.5 monolayers of InAs on GaAs, the formation of islands, 6 nm high and 20 nm in diameter, takes place. These QDs emit around $1.1 \mu\text{m}$, an inconvenient wavelength for single dot studies. We decrease the emission wavelength to 950 nm by introducing a further step in the growth [4]. This enables emission from single dots to be detected with a silicon CCD camera. The particular growth sequence involves growing 1 nm of GaAs on top of the QD layer and then annealing at the growth temperature of 520°C for about 1 min. During this step a reconfiguration of the material takes place forming laterally extended QDs [4]. The QD layer is overgrown by a 30 nm thick GaAs capping layer. A 116 nm thick AlAs/GaAs short period superlattice is then grown on top of the capping layer in order to inhibit electron transport to the surface. A 4 nm thick GaAs cap completes the heterostructure.

The concept of the device is to control the charge in the QDs through a vertical electric field. This field changes the electrostatic potential relative to that of the back contact. The equilibrium number of electrons in the dot changes as a function of potential. Because of the small size of the dots, there is a very pronounced Coulomb blockade [5]. In order to make a working device, a $4 \times 4 \text{ mm}^2$ piece of wafer material is pro-

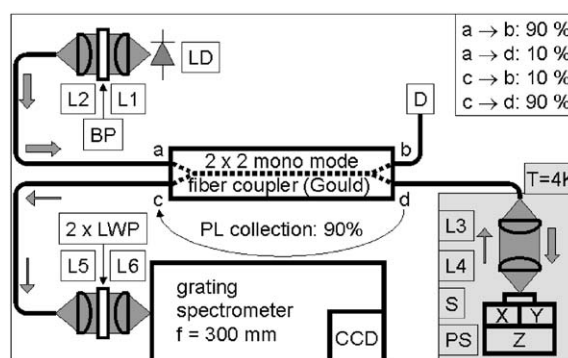


Fig. 1. Schematic of the experimental setup with components: LD: laser diode ($\lambda = 830 \text{ nm}$, $P_{\text{max}} = 5 \text{ mW}$); L1: aspheric lens (NA = 0.68, $f = 3.1 \text{ mm}$, Geltech); L2: aspheric lens (NA = 0.15, $f = 18.4 \text{ mm}$, Geltech); BP: band pass filter ($\lambda = 830 \text{ nm}$, BW = 40 nm, Coherent); D: detector (Si pin-photodiode, BPW34, Siemens); L3: aspheric lens (NA = 0.15, $f = 5.0 \text{ mm}$, Geltech); L4: aspheric lens (NA = 0.55, $f = 1.45 \text{ mm}$, Geltech); S: sample; PS: positioning stack (XYZ-positioner, Attocube Systems); L5: achromatic lens (NA = 0.25, $f = 50 \text{ mm}$, Thorlabs); L6: achromatic lens (NA = 0.13, $f = 100 \text{ mm}$, Thorlabs); LWP: long wave pass filter ($\lambda = 880 \text{ nm}$, $T \sim 80\%$ at $\lambda > 900 \text{ nm}$, NDC).

cessed to have an Ohmic contact to the back contact and a Schottky barrier at the surface.

The device is tested initially by measuring the capacitance between the gate and back contact. At low temperature, the capacitance shows charging peaks whenever electron tunneling takes place, and this is a definitive test of a working device.

The emission experiments were performed in a homemade miniature confocal microscope operating at 4.2 K. The microscope is mechanically stable with respect to changes in magnetic field and temperature and this unique feature allows us to measure the properties of a single QD for weeks at a time without adjusting the microscope. Optical access to the microscope is through an optical fiber, which transports both the excitation and the emission light. The microscope itself consists of a collimator and an objective, both miniature single aspheric lenses (L3 and L4 in Fig. 1). The sample is mounted on a positioning stack (PS), which allows a QD to be positioned both laterally and vertically with respect to the focus of the microscope. The positioner gives a coarse movement in steps of a few tens of nanometer with a range of 5 mm in the lateral directions and 8 mm in the

vertical direction and fine movement with a range of $0.5 \mu\text{m}$ at 4 K and $5 \mu\text{m}$ at 300 K in each direction.

For the photoluminescence (PL) measurement we use a diode laser emitting at 830 nm as excitation source (Fig. 1). The pump laser light (thick arrows in Fig. 1) is coupled into a mono-mode optical fiber using a collimating (L1) and focusing (L2) lens. A narrow band interference filter (BP) is used to block the broadband incoherent emission of the laser. The light is then transported through a 2×2 mono-mode fiber coupler, which operates as a beam splitter. Using connection a \rightarrow d in Fig. 1, 10% of the excitation signal is transmitted into the fiber leading to the microscope. The pump beam is collimated and focussed by the two aspheric lenses in the microscope (L3 and L4). The pump generates PL (thin arrows in Fig. 1). The PL is collected and focussed into the fiber by the same two lenses in the microscope. The objective is focussed for the emission wavelength in order to get the highest possible spatial resolution and the largest collection efficiency. With the microscope optimized for the PL at ~ 980 nm, the spatial resolution for the emission wavelength of 830 nm is about $2 \mu\text{m}$, larger than the diffraction limit because of achromaticity in the aspheric lenses. Most of the PL focussed into the fiber passes through the fiber coupler to the detection system consisting of a grating spectrometer and CCD camera. The spectrometer has a focal length of 300 mm, and spectral resolution 0.2 nm. At the entrance of the spectrometer we use a pair of long wave pass (LWP) filters to suppress the pump laser light which finds its way to exit c of the 2×2 coupler by reflection of the sample surface. The PL signal is then dispersed and detected by a silicon liquid nitrogen cooled CCD camera (30% quantum efficiency at 950 nm, negligible dark count signal, 2 counts rms readout noise). All the measurements are performed at liquid helium temperature with the miniature microscope cooled by exchange gas. The cryostat is equipped with a superconducting magnet with 2-in bore. The magnet is capable of providing a field of 9 T at 4.2 K.

3. Results

With the electric field effect structure we are able to investigate on the same QD excitons from uncharged

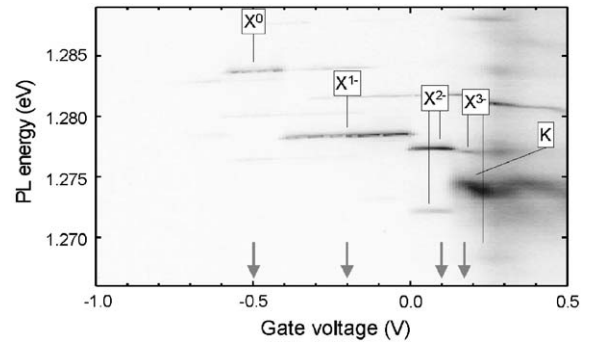


Fig. 2. Photoluminescence (PL) from a single QD as a function of gate voltage. The PL intensity is represented with a grey scale. The different plateaus represent the emission from uncharged (X^0), singly (X^{1-}), doubly (X^{2-}) and triply (X^{3-}) charged excitons. The arrows show the positions in gate voltage at which a magnetic field was applied. For X^{2-} and X^{3-} , the PL is split into two lines because there are two possible final states. The X^{3-} has two closely spaced initial states; the one with zero spin leads to the line labeled K.

up to three extra electrons by applying a gate voltage. Fig. 2 shows the gate voltage dependence of the PL of a single QD. We find that there are plateaus where the charge stays the same, with red shifts each time an electron is added to the dot [3]. This can be described as an excitonic Coulomb blockade. By setting the voltage in the middle of each plateau, we can determine the magnetic properties of each charged exciton. The magnetic dispersions of the differently charged excitonic complexes are shown in Fig. 3 up to a magnetic field of 9 T. For the X^0 , X^{1-} and X^{2-} exciton an unambiguous splitting of the emission line is observed resulting from the spin Zeeman effect. A quantitative analysis shows that the splitting depends linearly on magnetic field, and that to within the resolution of the experiment, the splitting is the same for all three charges [6]. We extract an excitonic g -factor $|g_{\text{ex}}| \sim 1.84$. Additionally, each spin branch in the magnetic dispersion has a diamagnetic shift, an energy increase quadratic in magnetic field [6]. We find that the quadratic coefficient is about $10 \mu\text{eV}/\text{T}^2$ for each charge from a fit to the data. This is a typical value for QDs of this sample indicating a wave function extent of ~ 5.5 nm. It is clear in Fig. 3 that the X^{3-} exciton shows a radically different behavior in magnetic field. There are two notable deviations from the

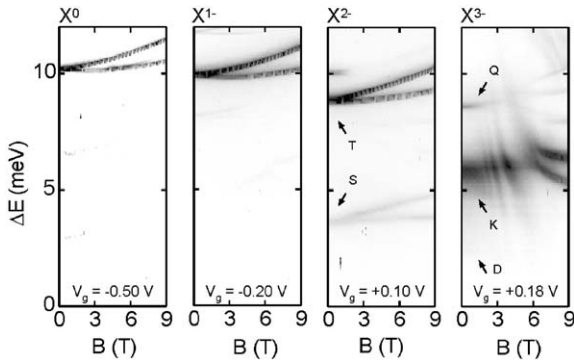


Fig. 3. Magnetic dispersion of X^0 , X^{1-} , X^{2-} and X^{3-} excitons. For X^{2-} , T and S label emission into the triplet and singlet final states, respectively. For X^{3-} , Q and D label emission into the quadruplet and doublet final states, respectively; K is the K-line.

spin-splitting and diamagnetic shift characteristic of the other excitons.

At zero magnetic field, the X^{3-} emission has two lines resulting from two possible final states after photon emission [3]. The initial state has spin 1; the final states either spin $\frac{3}{2}$ (Q) or $\frac{1}{2}$ (D). (We note that the D-emission is weaker than the quadruplet and hard to make out in Fig. 3.) The first significant point is that both the Q- and D-lines weaken rapidly for magnetic fields exceeding 2 T. The emission is replaced by a third emission line (K), appearing at an energy in between the Q- and D-lines. The second significant point in the magnetic dispersion of the X^{3-} exciton is that at magnetic fields larger than 2 T, the K-line shows a remarkable series of anti-crossings. The series of anti-crossings are periodic in inverse magnetic field, as shown in Fig. 4b. This behavior is not unique to this particular dot. Fig. 4a shows very similar X^{3-} behavior from a different QD in the same sample.

4. Discussion

We interpret the ‘collapse’ of the Q- and D- X^{3-} PL as a configuration change in the initial state. For a QD with high lateral symmetry, the X^{3-} initial state has spin 1 [3]. The two p electrons have the same spin as this lowers the energy through the exchange interaction. A magnetic field induces a splitting between the two p states such that at some point, it becomes energetically favorable for both electrons to

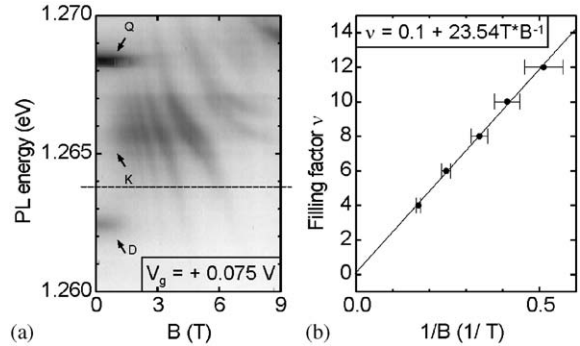


Fig. 4. (a) X^{3-} PL from a single dot versus magnetic field at 4.2 K. The dot is different from the dot in Fig. 3. The dashed line indicates the PL energy at which the periodicity of the PL was determined. (b) Plot of index versus inverse magnetic fields at the resonances in the PL intensity. The index changes by two from one maximum to the next, and is therefore treated like the filling factor in the analysis of Shubnikov–de Haas oscillations.

occupy the lower p state forming a spin 0 system. Once this has occurred, there is just one final state, so that the PL ‘collapses’. At higher fields, there is a periodicity in $1/B$, which at first sight is reminiscent of Shubnikov–de Haas oscillations in the conductivity of a two-dimensional (2D) electron gas. We pursue this analogy by considering the hypothesis that the period in $1/B$ can be used to obtain a 2D carrier density. We perform the analysis by taking a section at constant PL energy (dashed line in Fig. 4a) and calculating the inverse fields for the maxima in PL intensity, in complete analogy to the analysis of Shubnikov–de Haas oscillations. Fig. 4b shows the result of this analysis, a plot of filling factor ν versus $1/B$. The slope of 23.54 T gives a 2D electron density within this hypothesis of $5.69 \times 10^{11} \text{ cm}^{-2}$. We now compare this value to that obtained from the magneto-capacitance on the same sample. This is an ensemble measurement and therefore gives an average 2D electron concentration. At large positive voltages there are pronounced Shubnikov–de Haas oscillations in the magneto-capacitance as shown in Fig. 5a with each minimum labeled with the corresponding filling factor. We calculate an electron density n_s of $3.4 \times 10^{11} \text{ cm}^{-2}$. The large voltage causes the wetting layer to be occupied with electrons and it is well known that electrons in the wetting layer are quasi-2D. The electron density depends on the gate

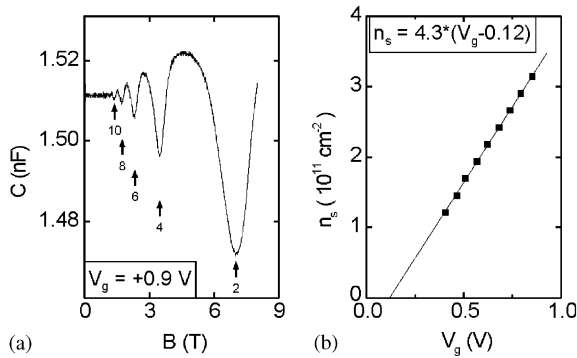


Fig. 5. (a) Magneto-capacitance measurement on an ensemble of QDs. The arrows indicate the points at which an integral number of Landau levels are completely occupied and are labeled by the filling factor. (b) 2D electron density versus gate voltage as determined from the magneto-capacitance.

voltage, as shown in Fig. 5b. In particular, there is an onset voltage of +0.12 V below which the wetting layer is unoccupied. There are therefore two compelling reasons why the hypothesis of a 2D electron gas fails to explain the anti-crossings in the X^{3-} PL. First, the PL predicts a density, which is higher than can be achieved in the wetting layer even at large positive voltages. Secondly, the anti-crossings in the X^{3-} PL arise even at gate voltages where the wetting layer is not occupied with electrons (Fig. 4a) or at low 2D electron density (Fig. 3 last plot). Instead a different mechanism must induce the anti-crossings.

The mechanism we propose depends on the s state vacancy after photon emission. This enables an Auger process to take place between the two p electrons and the remaining s electron. One p electron occupies the vacancy in the s state, allowing the second p electron to be promoted to Landau-like levels at higher energy. The anti-crossings demonstrate that this Auger process

is coherent such that the system can be thought to oscillate between localized QD character and extended Landau level-like character. The model is consistent with the experimental results as it predicts a $1/B$ periodicity even without occupation of the Landau levels in the initial state. A quantitative model of the process will be presented elsewhere.

5. Conclusion

We have presented a novel technique for performing single dot spectroscopy at low temperature and at high magnetic fields. The microscope is fiber based and has the advantage that the spot position does not move with respect to the sample as a function of magnetic field. Some example results on the magneto-PL from charged excitons in an individual dot are presented. The neutral, singly and doubly charged excitons exhibit a spin Zeeman effect and diamagnetic shift in a magnetic field which are characteristic of a strongly localized emitter. We find however that the triply charged exciton behaves quite differently, exhibiting a series of anti-crossings periodic in $1/B$. We demonstrate that this cannot be related to Shubnikov–de Haas oscillations of electrons in the wetting layer. The results therefore demonstrate that a hybridisation of QD and unoccupied Landau levels takes place.

References

- [1] C. Santori, et al., Nature 419 (2002) 594.
- [2] M. Bayer, et al., Phys. Rev. B 65 (2002) 041308.
- [3] R.J. Warburton, et al., Nature 405 (2000) 926.
- [4] J.M. Garcia, et al., Appl. Phys. Lett. 71 (1997) 2014.
- [5] R.J. Warburton, et al., Phys. Rev. B 58 (1998) 16221.
- [6] C. Schulhauser, et al., Phys. Rev. B 66 (2002) 193303.